

Energy dissipation rates in low- Re_m MHD turbulence with mean shear: Results for channel flow with spanwise field

D. Krasnov¹, O. Zikanov², J. Schumacher¹ and T. Boeck¹

¹ *Fakultät Maschinenbau, Technische Universität Ilmenau,
Postfach 100565, 98684 Ilmenau, Germany*

² *University of Michigan-Dearborn, 48128 MI, USA*

We examine the changes in kinetic energy dissipation of a turbulent channel flow caused by a spanwise magnetic field. The numerical study is based on our simulation data from [1] obtained by direct and large eddy simulations. We find that the Joule dissipation can exceed the viscous dissipation in the weakly dissipative bulk region, but remains comparatively small in the turbulence-generating near-wall region.

Introduction This paper continues our recent analysis [1] of turbulent channel flow in a steady magnetic field imposed in the spanwise (parallel to the walls but normal to the mean flow) direction. The magnetic Reynolds number is assumed small, and the problem is solved in the framework of the quasi-static approximation [2]. We are interested in this problem because the channel flow with spanwise magnetic field represents the simplest natural flow configuration, in which we can study turbulence under the combination of two conditions common in industrial and laboratory flows of liquid metals: imposed magnetic field and mean shear. At the same time, the transformation of turbulent fluctuations occurs without direct interaction between the mean flow and the magnetic field and without the dominating influence of Hartmann boundary layers.

A thorough study of the flow at high hydrodynamic Reynolds number $Re \equiv UL/\nu =$ and moderate Hartmann number $Ha \equiv BL(\sigma/\rho\nu)^{1/2}$ was conducted in [1]. Here, U and L are the typical velocity and length scales, chosen in our case as the centerline velocity of the laminar flow and half the channel width, B is the strength of the applied magnetic field, and σ , ρ and ν are the electric conductivity, density, and kinematic viscosity of the fluid. The results confirmed and extended the conclusions of the earlier experimental work [3] and numerical simulations at low Reynolds number [4]. We found that the main effect of the magnetic field is the suppression of turbulent fluctuations, particularly pronounced in the wall buffer regions, where the fluctuations are generated by strong mean shear. The resulting reduction of the turbulent momentum transport in the wall-normal direction decreases the wall friction drag and transforms the mean flow profile, which becomes steeper, acquires higher centerline velocity, and loses the zone of the logarithmic layer behavior.

Analyzing the anisotropy of turbulent fluctuations, we found that the elongation of flow structures in the direction of the magnetic field observed in homogeneous zero-shear turbulence (see, e.g. [5, 6, 7]) appears only in a weak form and only in the central area of the channel. It should be stressed that all the results of [1] were obtained at moderate strength of the magnetic field, at $Ha \leq 30$ for $Re = 10^4$ and $Ha \leq 40$ for $Re = 2 \times 10^4$. Stronger magnetic fields lead to an interesting intermittent flow regime, in which turbulent states alternate with periods of nearly laminar behavior [8].

The combination of the two factors, the mean shear and the imposed magnetic field, also renders the channel flow an excellent configuration for testing computational models of turbulence, in particular LES models. This was done in [1] using the *a-posteriori* comparison with the results of high-resolution DNS. In agreement with the earlier studies, such as [6, 9, 10], the dynamic Smagorinsky model was shown to accurately reproduce the MHD flow transformation.

In the present paper, we extend the investigation by considering the viscous and magnetic (Joule) dissipations. The databases generated in the LES and high-resolution DNS computations [1] are employed to analyze the effect of the magnetic field on the dissipation rates in various zones of the flow. An important goal of the study is to interpret the observed flow transformation in terms of the local energy balance. We provide further verification of the dynamic Smagorinsky model by analyzing the accuracy, with which the model reproduces the dissipation rates. Such accuracy is generally considered one of the most important characteristics of an LES model's performance.

Equations and numerical method We consider the flow of an incompressible, electrically conducting fluid in a plane channel between two insulating walls located at $z = \pm L$. The flow is driven by a streamwise pressure gradient and submitted to a constant spanwise magnetic field $\mathbf{B} = B\mathbf{e}_y$. The mean flow velocity U_q is kept constant in the simulations. The dimensional governing equations and boundary conditions for the velocity field u_i , pressure p , electric current density J_i and electric potential ϕ are

$$\frac{\partial u_i}{\partial t} + u_j \frac{\partial u_i}{\partial x_j} = -\frac{1}{\rho} \frac{\partial p}{\partial x_i} + \frac{1}{\rho} \frac{\partial}{\partial x_j} (\tau_{ij} + \tau_{ij}^a) + \frac{1}{\rho} \epsilon_{ijk} J_j B_k, \quad (1)$$

$$J_i = \sigma \left(-\frac{\partial \phi}{\partial x_i} + \epsilon_{ijk} u_j B_k \right), \quad (2)$$

$$\frac{\partial u_i}{\partial x_i} = \frac{\partial J_i}{\partial x_i} = 0, \quad (3)$$

$$u = v = w = \frac{\partial \phi}{\partial z} = 0 \quad \text{at } z = \pm L. \quad (4)$$

In these equations, $\tau_{ij} = 2\rho\nu S_{ij}$ is the resolved viscous stress tensor, where $2S_{ij} = \partial u_i/\partial x_j + \partial u_j/\partial x_i$ is the rate-of-strain tensor. The additional subgrid stress tensor τ_{ij}^a , which appears in LES computations, is given by $\tau_{ij}^a = 2\rho\nu_T \bar{S}_{ij}$. It is computed using the local filtered rate of strain tensor \bar{S}_{ij} , with the eddy viscosity ν_T determined by the dynamic Smagorinsky model with averaging in horizontal planes.

Variables are made non-dimensional by the laminar centerline velocity U , half-channel width L and ULB (for ϕ). The non-dimensional parameters are Re and Ha . The problem is solved numerically in a domain with the periodicity lengths $L_x/L = 2\pi$ and $L_y/L = \pi$. The pseudo-spectral numerical method is described in [1, 11]. The numerical resolution is $N_x \times N_y \times N_z = 256^3$ collocation points in the simulations with $Re = 10^4$ and $512^2 \times 256$ collocation points at $Re = 2 \times 10^4$. The spatially filtered equations for LES are solved using 64^3 and 128^3 collocation points at $Re = 10^4$ and $Re = 2 \times 10^4$, respectively.

The equation of the local kinetic energy balance is formed from the momentum equation (1) by multiplying it by the velocity vector \mathbf{u} , making use of Ohm's law, and rearranging such that the energy transport terms are entirely separated from

the local dissipation terms. The result is the equation

$$\frac{\partial e}{\partial t} = -\nabla \cdot \mathbf{N} - \varepsilon_{\text{visc}} - \varepsilon_{\mu} - \varepsilon_{\text{sgs}}, \quad (5)$$

where $e = u^2/2$ is the specific kinetic energy,

$$\varepsilon_{\text{visc}} \equiv \tau_{ij} S_{ij} / \rho \quad (6)$$

is the viscous dissipation rate, and

$$\varepsilon_{\mu} \equiv J^2 / \sigma \rho \quad (7)$$

is the Joule dissipation rate. The additional dissipation rate due to the subgrid stresses is

$$\varepsilon_{\text{sgs}} \equiv \tau_{ij}^a \bar{S}_{ij} / \rho. \quad (8)$$

\mathbf{N} is the energy flux vector due to convective transport, pressure force, friction force, subgrid stresses, and Lorentz force. It is given by

$$\rho N_i = \rho u_i \left(\frac{u^2}{2} + \frac{p}{\rho} \right) - u_i \tau_{ij} - u_i \tau_{ij}^a - \phi J_i. \quad (9)$$

In the case of DNS, the subgrid stress contribution is absent from all of the above equations.

Results We first consider the spatial structure of the Joule dissipation field. Fig. 1 illustrates the trend observed in our earlier paper [1] for the velocity field: a stronger magnetic field leads to turbulence suppression and smoother, larger structures.

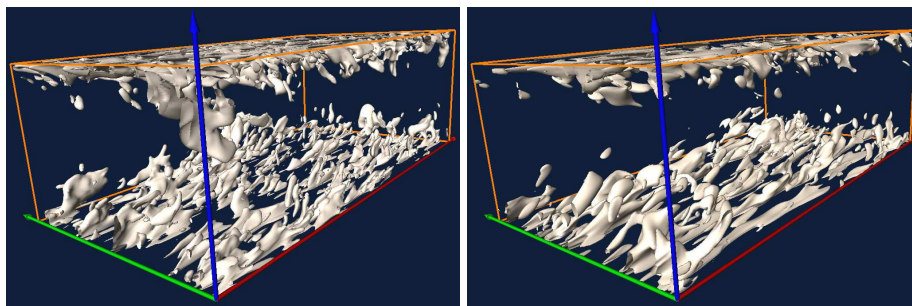


Figure 1: Iso-surfaces $\varepsilon_{\mu} / \varepsilon_{\mu}^{rms} = 2$ of the Joule dissipation rate for $Ha = 10$ (left) and $Ha = 30$ (right) from DNS with $Re = 10000$. Snapshots of the entire computational domain are shown.

For further analysis, we focus on the average distributions of dissipation rates and their transformation by the magnetic field. The averaging is performed in x - y -planes and in time over several convective times L/U . We begin with the demonstration that LES reproduces the dissipation rates with satisfactory accuracy. Fig. 2 shows close agreement between the mean profiles of the viscous dissipation rate from DNS and the sum of viscous and sub-grid scale dissipation rates from LES in the non-magnetic cases. Figs. 3(a,b) show similar agreement for the cases of the strongest magnetic fields realized in the simulations. For the latter two cases, the Joule dissipation rates shown in Figs. 3(c,d) also show good

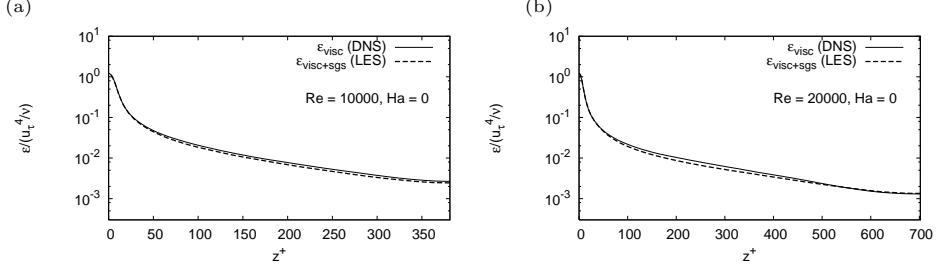


Figure 2: Time-averaged profiles of $\varepsilon_{\text{visc}}$ for (a) $Re = 10000$ at $Ha = 0$ and (b) $Re = 20000$ at $Ha = 0$. In case of LES the total viscous dissipation $\varepsilon_{\text{visc}+\text{sgs}}$ is plotted. Normalization is by u_τ^4/ν obtained for each case from DNS. The distance z^+ from the wall is measured in units of the friction length ν/u_τ .

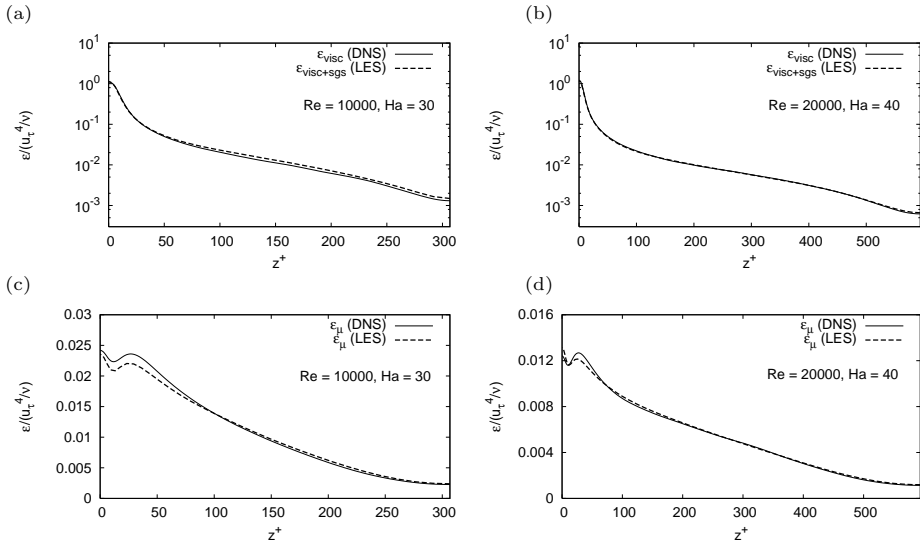


Figure 3: Time-averaged profiles of $\varepsilon_{\text{visc}}$ and ε_μ for (a,c) $Re = 10000$ at $Ha = 30$ and (b,d) $Re = 20000$ at $Ha = 40$. In case of LES the total viscous dissipation $\varepsilon_{\text{visc}+\text{sgs}}$ and the resolved part of the Joule dissipation $\varepsilon_\mu^{\text{resolved}}$ are plotted. Normalization is by u_τ^4/ν obtained for each case from DNS.

agreement. It should be mentioned that the comparison should, in principle, be done between the LES and filtered DNS results. Filtering was not performed in our analysis. Unlike the viscous dissipation, the Joule dissipation rate varies with the length scale in about the same way as the kinetic energy, and the Joule dissipation in the subgrid scales should therefore be quite small. The slightly larger discrepancies in ε_μ near the wall at $Re = 10^4$ in Fig. 3(c) are most likely caused by a comparatively coarser LES resolution than for $Re = 2 \times 10^4$ (Fig. 3(d)). In any case, our LES results are quite satisfactory for the mean profiles of the dissipation rates. This observation is further supported by Table 1, which shows that the fraction of the Joule dissipation relative to the total dissipation is well represented in the LES model.

Non-magnetic turbulent channel flows are characterized by local equilibrium

Run	Ha	$\varepsilon_\mu/\varepsilon_{\text{tot}}$	$\varepsilon_{\text{sgs}}/\varepsilon_{\text{tot}}$	Run	Ha	$\varepsilon_\mu/\varepsilon_{\text{tot}}$	$\varepsilon_{\text{sgs}}/\varepsilon_{\text{tot}}$
$Re = 10000$				$Re = 20000$			
LES	10	0.020	0.116	LES	20	0.042	0.113
LES	20	0.077	0.095	LES	30	0.088	0.099
DNS	30	0.158	0.0	DNS	40	0.142	0.0
LES	30	0.154	0.067	LES	40	0.147	0.080

Table 1: Time- and volume-averaged subgrid-scale and Joule dissipation rates relative to the total energy dissipation rate $\varepsilon_{\text{tot}} = \varepsilon_{\text{visc}} + \varepsilon_\mu + \varepsilon_{\text{sgs}}$.

between kinetic energy production and dissipation and by the approximate relation $\varepsilon_{\text{visc}} \sim 1/z^+$ in the logarithmic layer [12]. The product $z^+ \varepsilon_{\text{visc}}$ should therefore be approximately constant. Fig. 4 shows this quantity as found in our DNS computations. We can identify a plateau for $Re = 2 \times 10^4$ in both magnetic and non-magnetic cases, although it is shown in [1] that the mean velocity profile for $Ha = 40$ deviates significantly from the logarithmic law. For $Re = 10^4$ the quantity $\varepsilon_{\text{visc}}$ decays somewhat faster than $1/z^+$ in the non-magnetic as well as the magnetic case, and the plateau is therefore not observed.

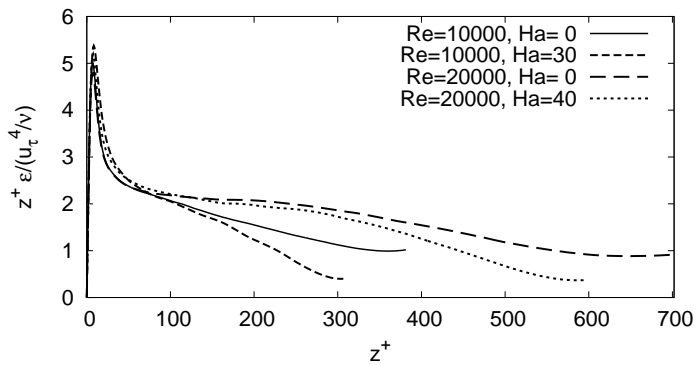


Figure 4: Compensated viscous dissipation $z^+ \varepsilon_{\text{visc}}$ from DNS for $Re = 10000$ at $Ha = 0, 30$ and $Re = 20000$ at $Ha = 0, 40$. The plots are continued up to the middle of the channel, which varies because of different friction lengths ν/u_τ .

The systematic trends in the behavior of the dissipation rates with increasing magnetic field are illustrated in Fig. 5 by the LES data obtained at $Re = 10^4$. The results for $Re = 2 \times 10^4$ are qualitatively identical and, therefore, omitted. Figs. 5(a,b) show that the viscous dissipation rate is significantly reduced by the magnetic field near the wall and in the middle of the channel. The reduction at the walls is expected because of the suppression of the intensity of the turbulent fluctuations observed in [1]. The reduction in the middle is less significant for the overall level of dissipation since this region contributes very little, but the relative change in $\varepsilon_{\text{visc}}$ by a factor of about 3.3 from $Ha = 0$ to $Ha = 30$ is larger than at the wall. The Joule dissipation rate shown in Fig. 5(c) increases significantly with Ha but without much change in the profile shape. The subgrid-scale dissipation rate in Fig. 5(d) decreases significantly from $Ha = 0$ to $Ha = 30$, as can be expected from the magnetic damping of the turbulence and the corresponding depletion of the subgrid scales.

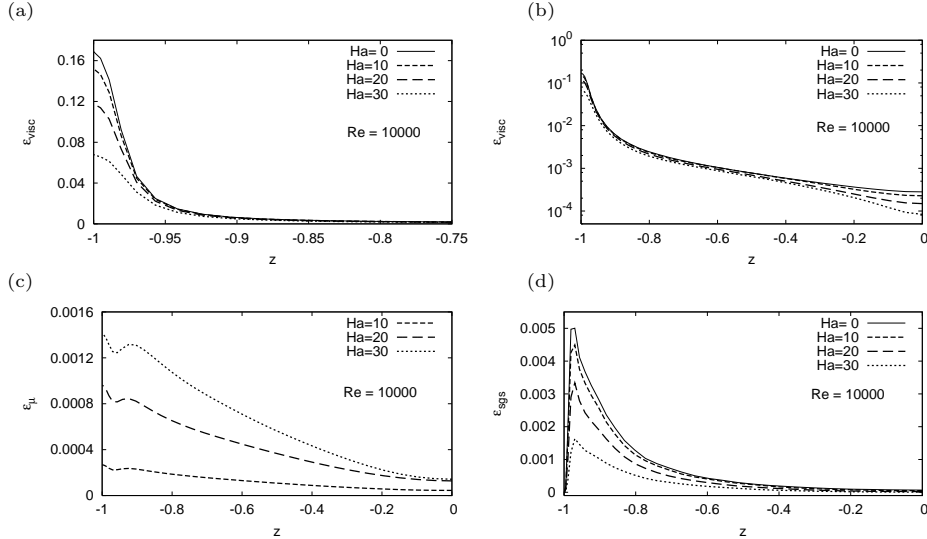


Figure 5: Horizontally and time-averaged rates of (a,b) viscous, (c) Joule and (d) subgrid-scale dissipation rates from LES for different Ha at $Re = 10000$. The viscous term is shown for the near-wall region (a) and, to facilitate the comparison in the bulk region, in log-scale (b). Quantities are normalized by U_q^3/L , which is identical for the different Ha .

The relative contributions of the dissipation rates are compared in Fig. 6, which shows mean profiles calculated in LES for $Re = 10^4$ and $Re = 2 \times 10^4$. At low Ha , the contribution from the Joule dissipation rate is everywhere smaller than that of the viscous dissipation, but for the highest Ha , the Joule dissipation becomes comparable or even larger than $\varepsilon_{\text{visc}}$ in the bulk region. The overall contributions are compared in Table 1. The contribution of the subgrid-scale dissipation diminishes considerably in the bulk with increasing Ha , especially for $Re = 2 \times 10^4$ with its larger number of grid points. The overall contribution of the subgrid-scale dissipation remains nonetheless of the order of 10%.

In conclusion we remark that both the Joule and viscous dissipation rates peak at the wall. The Joule dissipation rate attains a local maximum in the buffer region, where the turbulence is primarily generated. The shape of the Joule dissipation profile is not much affected by the strength of the magnetic field. Its contribution to the total dissipation remains fairly modest, but it can exceed the viscous dissipation locally (in the bulk) before the intermittent dynamics described in [8] appears at larger Ha . The contribution of the subgrid-scale dissipation and, thus, the importance of the LES modeling, diminishes with the strength of the magnetic field, but remains significant even at the strongest field at which a continuous turbulent state is maintained.

Acknowledgements. TB, DK and OZ acknowledge financial support from the Deutsche Forschungsgemeinschaft (Emmy-Noether grant Bo 1668/2-3 and Gerhard-Mercator visiting professorship program). Computer resources were provided by the computing centers of TU Ilmenau and the Forschungszentrum Jülich (NIC).

REFERENCES

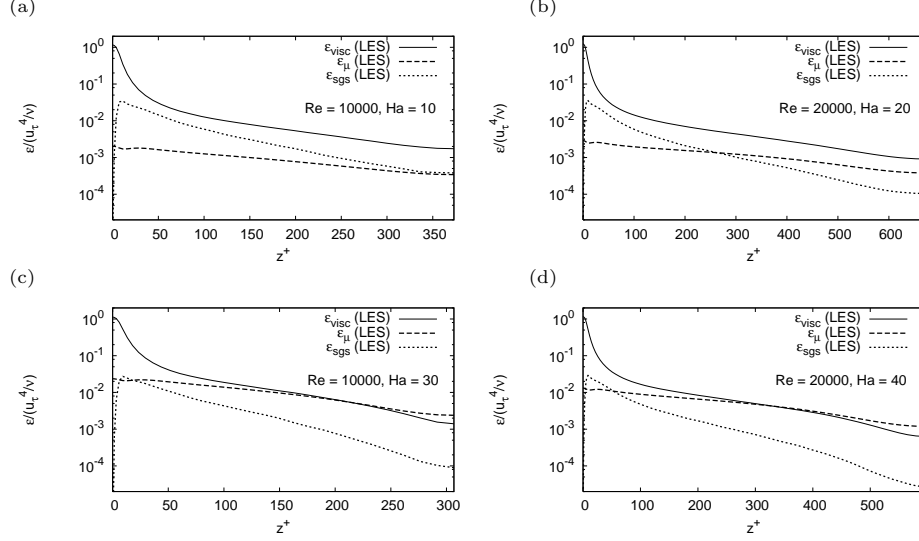


Figure 6: Mean profiles of the dissipation rates obtained from LES for $Re = 10000$ (left) and $Re = 20000$ (right) at different Ha . Normalization is by u_τ^4/ν obtained for each case from DNS.

1. D. KRASNOV, O. ZIKANOV, J. SCHUMACHER, AND T. BOECK. Magnetohydrodynamic turbulence in a channel with spanwise magnetic field. *Phys. Fluids*, vol. 20, (2008), 095105.
2. H. ROBERTS. *An Introduction to Magnetohydrodynamics*. Longmans Green (1967).
3. A. D. VOTSISH AND YU. B. KOLESNIKOV. An experimental investigation of two-dimensional turbulence characteristics in a plane channel with an azimuthal magnetic field. *Magnetohydrodynamics*, vol. 13, (1977), pp. 27–30.
4. D. LEE AND H. CHOI. Magnetohydrodynamic turbulent flow in a channel at low magnetic Reynolds number. *J. Fluid Mech.*, vol. 429, (2001), pp. 367–394.
5. O. ZIKANOV AND A. TCESS. Direct numerical simulation of forced MHD turbulence at low magnetic Reynolds number. *J. Fluid Mech.*, vol. 358, (1998), pp. 299–333.
6. B. KNAEPEN AND P. MOIN. Large-eddy simulation of conductive flows at low magnetic Reynolds number. *Phys. Fluids*, vol. 16, N5, (2004), pp. 1255–1261.
7. A. VOROBEV, O. ZIKANOV, P. A. DAVIDSON, AND B. KNAEPEN. Anisotropy of magnetohydrodynamic turbulence at low magnetic Reynolds number. *Phys. Fluids*, vol. 17, (2005), 125105.
8. T. BOECK, D. KRASNOV, A. TCESS, AND O. ZIKANOV. Large-Scale Intermittency of Liquid-Metal Channel Flow in a Magnetic Field. *Phys. Rev. Lett.*, vol. 101, (2008), 244501.
9. A. VOROBEV AND O. ZIKANOV. Smagorinsky constant in LES modeling of anisotropic MHD turbulence. *Theor. Comp. Fluid Dyn.*, vol. 22, N3-4, (2008), pp. 317–325.
10. I. E. SARRIS, S. C. KASSINOS, AND D. CARATI. Large-eddy simulations of the turbulent Hartmann flow close to the transitional regime. *Phys. Fluids*, vol. 19, (2007), 085109.
11. D. S. KRASNOV, E. ZIENICKE, O. ZIKANOV, T. BOECK, AND A. TCESS. Numerical study of the instability of the Hartmann layer. *J. Fluid Mech.*, vol. 504, (2004), pp. 183–211.
12. S. B. POPE. *Turbulent Flows*. Cambridge (2000).